The role of plastin 3 in collective invasion of MMTV-PyMT breast cancer organoids

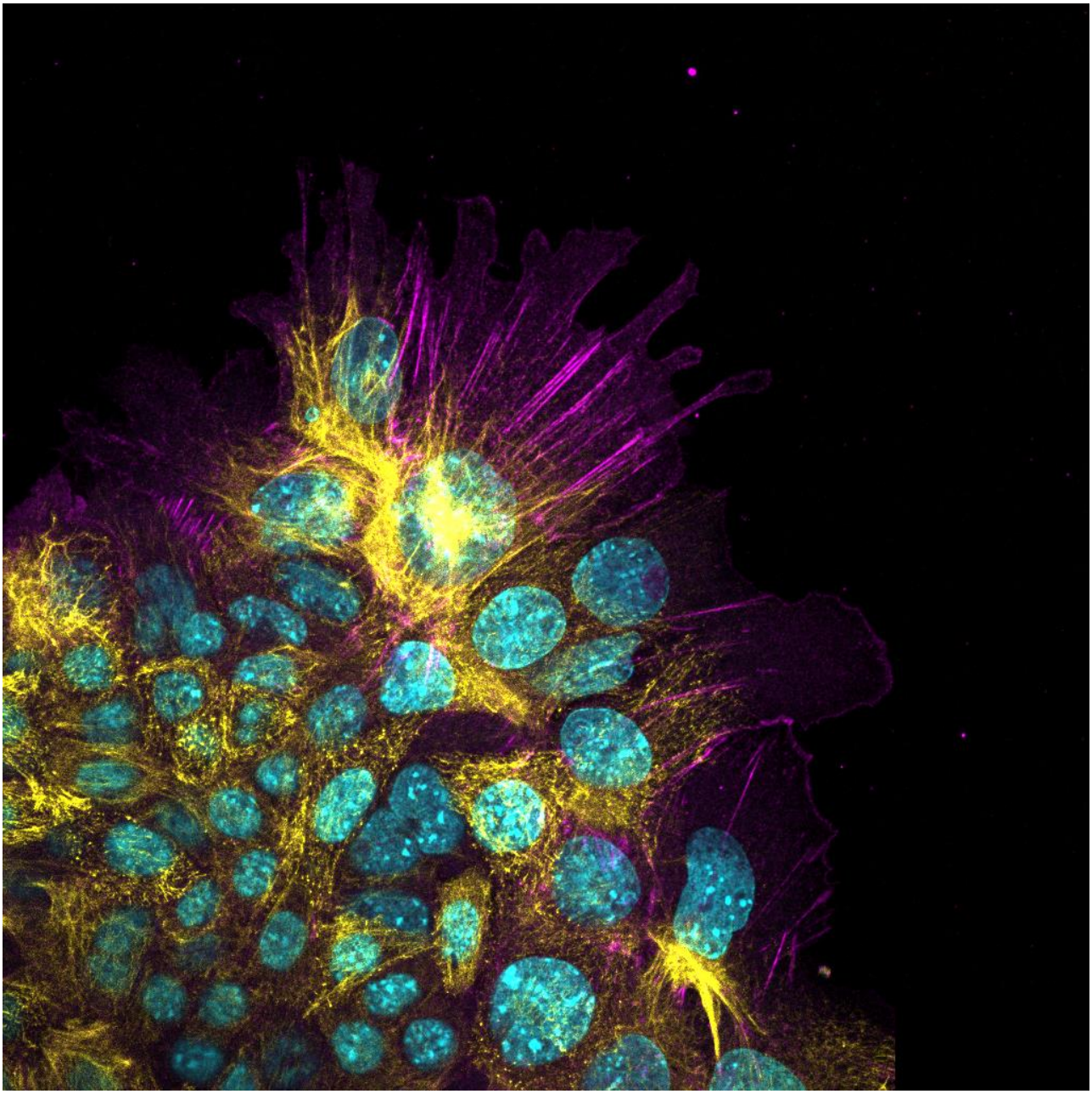

Report Major Internship | Leonieke den Outer | November 24, 2021

Title report: The role of plastin 3 in collective invasion of MMTV-PyMT breast cancer organoids

Report by: Leonieke den Outer

Student number: 5876621

Date: November 24, 2021

Master: Biology of Disease

Supervisor: Dr. Antoine A. Khalil

Examiner: Dr. Johan de Rooij

Second reviewer: Dr. Martijn Gloerich

Institution: University Medical Center Utrecht

Department: Center for Molecular Medicine, Molecular Cancer Research

Index

Abstract

Most invasive ductal carcinomas (IDCs) spread into the surrounding extracellular matrix (ECM) in groups of cells, a process termed collective invasion. Collective invasion of several IDCs is initiated and driven by cells with basal-like characteristics such as the expression of keratin 14 (K14). Basal-like cells that are located at the tumor-ECM interface acquire protrusive and motile behavior and become the leader cells of collective invasion. Previous single cell mRNA sequencing from our lab showed that Plastin 3 (PLS3), an F-actin binding and -bundling protein, is upregulated in basal-like cells during collective invasion. Whereas high PLS3 levels are associated with worse prognosis in breast cancer patients, the role of PLS3 in breast tumor progression, especially during collective invasion, remains unclear. Using PLS3 immunohistochemistry of IDC samples from the Human Protein Atlas Project, we found that PLS3 was upregulated at the tumor-ECM interface of cancer cell groups invading into the breast tissue. Furthermore, with the use of MMTV-PyMT breast cancer organoid mouse model and immunofluorescence (IF) confocal imaging in 3D and on 2D collagen 1, we found that PLS3 is upregulated when basal-like cells are located at the leader cell position in invading strands and migrating monolayers, respectively. To study the functional role of PLS3 in leader cell guided invasion, we interfered with its expression by doxycyclin-inducible PLS3 knockdown in MMTV-PyMT organoids. Our preliminary data shows that 62% knockdown of PLS3 did not affect invasion in 3D collagen 1. Additional experiments are required to determine the requirement of PLS3 in cancer leader cell function and collective invasion. Overall, our findings demonstrate that PLS3 is expressed at the tumor-ECM interface and is upregulated in basal-like leader cells during collective invasion.

Layman's summary

Breast cancer is one of the most common cancer in women worldwide. The spreading of cancer cells from the primary tumor to different organs in the body and the formation of a secondary tumor there (metastasis), is the major cause of patient's death. In order to spread to other organs, the cancer cells first need to invade their surrounding tissue. Breast cancer cells do this in groups, in a process called collective invasion. Here the cancer cells that are present at the outer layers of the tumor (basal-like cells), are the first to start the process. A first cell, called a leader cell, starts and guides the direction and other cells follow by keeping cell-to-cell contact. In this way, strands of multiple cells one after another are formed that extend into the tissue. Previous research done in our lab showed that basal-like cells acquire certain changes in genetic composition before they become an invasive leader cell. One of these genes is *plastin 3* (PLS3). The *PLS3* gene encodes for a protein that is involved in supporting the skeleton of the cell (cytoskeleton). The support of the cytoskeleton is essential for cells to be able to protrude and move in a directional way. However, what is not known, is the role of PLS3 in leader cell functioning during collective invasion. Using 3D clusters of mouse breast tumors, called organoids, we studied the role of PLS3 in basal-like cells during invasion. Using microscopy, we identified that PLS3 is mostly present in the basal-like cells at the sites where the cancer cells make contact with the surrounding tissue. And PLS3 was even more expressed in the leader cells of the invasive strands. The upregulation of PLS3 at the sites where cancer cells contact the surrounding tissue was also observed in collective invasion in patient samples. In addition, we made a special organoid line where the expression of PLS3 was genetically reduced. Preliminary results show that reduction of PLS3 expression did not affect invasion. However, PLS3's role could be subtle and needs to be studied in more detail. On further research, PLS3 might provide a better way of understanding the molecular mechanism that lies beneath breast cancer invasion and metastasis.

Introduction

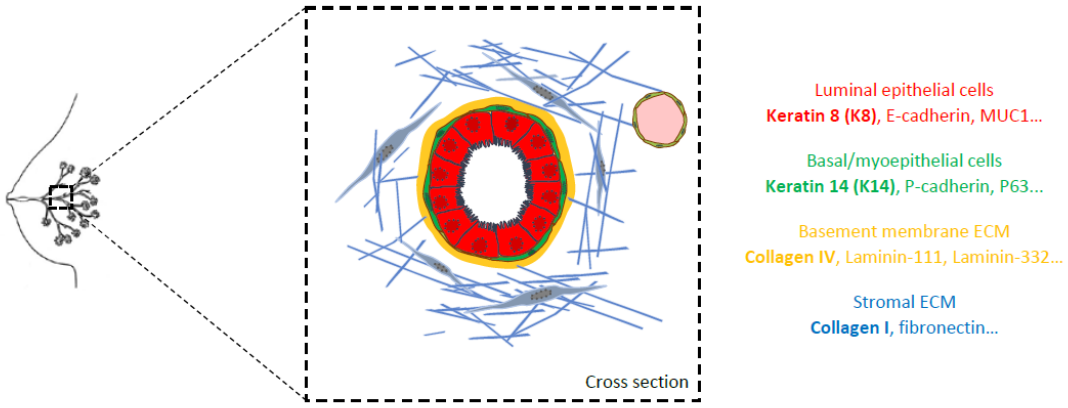

Figure 1 – Schematic display of a cross section of a breast ductus.

The normal breast constitutes of a network of branching ducts (Fig. 1). The ducts are comprised of two cellular layers (Fig.1, zoom in). Luminal epithelial cells layer the inside of the duct and produce and secrete the milk into the lumen.[1] The luminal epithelial cells are surrounded by myoepithelial (basal) cells, contractile cells.[1] At the molecular level, the two cell types express different cytokeratins, which are intermediate filaments that are important for mechanical stress response in epithelial cells. Cytokeratin 8 (K8) is a marker for luminal epithelial cells, whereas cytokeratin 14 (K14) is a marker for basal cells.[2] Additionally, a basement membrane, consisting of extracellular matrix (ECM) molecules such as collagen IV and laminin, surrounds the duct and prevents the epithelial cells from making contact with the stromal ECM.[3] The duct is within stromal ECM that consists of collagen 1, collagen III and fibronectin as major ECM proteins (see Fig.1).[4]

The mammary gland tissue is highly dynamic and undergoes many structural changes during the menstruation cycle and pregnancy.[5] Because of these cyclic changes, breast tissue is susceptible for cellular transformation of the luminal cells, making it the most common cancer in women worldwide.[6]

Upon tumor formation, the organized tissue structure with apicobasal polarity is disrupted.[7–10] Luminal epithelial cells start to proliferate in an uncontrolled manner and fill the ducts causing the lumen to disappear (Fig.2). At this stage the tumor still maintains its myoepithelial coverage and basement membrane and is called a ductal carcinoma in situ (DCIS).[11] However, this changes into an malignant invasive ductal carcinoma (IDC) whenever the luminal cells breach the basement membrane and start spreading into the surrounding stromal ECM.

It is believed that in many IDCs, luminal cells acquire basal-like characteristics in order to become invasive.[12] Basal cell characteristics include the expression of K14, K5, p63 and P-cadherin.[8] At the tumor-ECM interface, the basal-like cells protrude into the ECM and acquire leader cell characteristics that drive the initiation and guidance of invasion (Fig.2). These cells are called leader cells.[13,14] Leader cells maintain their cell-to-cell junctions with follower cells and form in this way a cohesive group that migrates in a directional manner, termed collective invasion (Fig.2).[15] Collective invasion occurs often as multicellular strands that protrude into the stromal ECM by adhering and pulling on ECM molecules such as collagen 1.[16,17] This guides the spread into the surrounding tissue and facilitates the accessibility of cancer cells to the neighboring

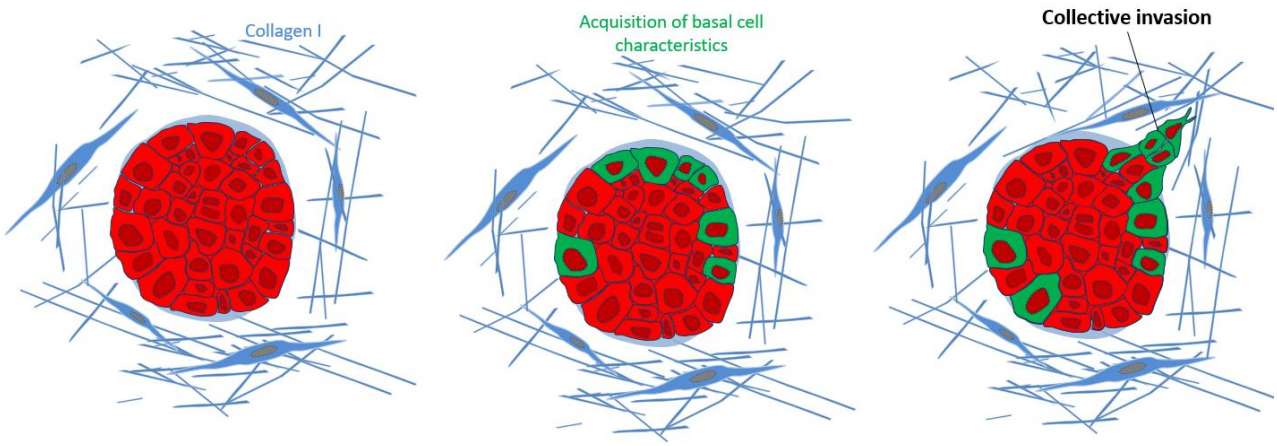

Figure 2 – Cartoon of collective invasion. Luminal cells (red) and basal cells (green) are shown.

blood vessels. After intravasation into the blood vessels, cancer cells within the circulation may reach other organs where they form secondary tumors, metastasis. Thus, collective invasion represents an essential step in distant metastasis.

Our interest lays in the interaction of the basal-like cells with collagen 1. Single cell mRNA sequencing of MMTV-PyMT breast cancer organoids, previously performed in our lab showed that collagen 1 promotes a specific transcriptional program in the basal-like cells. Certain genes that were upregulated were important for cytoskeletal organization and protrusions, such as plastin 3 (PLS3). PLS3 gene is located on the X-chromosome and its mostly expressed in cells from solid tissues.[18] The main function of PLS3 is F-actin binding and -bundling. Binding of the two actin-binding domains (ABD) of PLS3 to actin promotes the formation of a bundle with a center-to-center distance of ~120 Å between the filaments, making the actin filaments into stronger aligned bundels.[19] As an F-actin binding and -bundling protein, PLS3 plays a role in several processes dependent on F-actin dynamics, such as cell motility, cell division and others.[20] PLS3 binding to actin is essential at the leading edge where lamellipodia and filopodia are formed during cell migration.[21,22] Moreover, PLS3 reinforces membrane protrusions and promotes cell migration by bridging matrix gaps.[23]

Cells use focal adhesions to connect their actin network to the underlying ECM. First with small lamellipodia and filopodia, later these adhesions are strengthened by stress fibers and other myosin II-dependent tensions.[24] P

PLS3 levels in the cell are tightly regulated and balanced in the cell. Several cancers are associated with increased levels of PLS3, whereas deletions or loss-of-function mutations in PLS3 could cause osteoporosis.[25] In cancer, PLS3 has been associated with aggressive cancer cell behavior. In colorectal cancer, PLS3 is highly expressed in circulating tumor cells (CTCs) that undergo the epithelial-mesenchymal transition (EMT).[26] In gastric cancer and non-small cell lung cancer (NSCLC), high expression levels of PLS3 are associated with poor prognosis.[27,28] And in liver cancer, downregulation of PLS3 increases the sensitivity to cisplatin, a chemotherapeutic cancer drug.[29] Regarding breast cancer, PLS3 is overexpressed in two-third of CTCs isolated from breast cancer patients and high levels are associated with poor survival.[30] Moreover, silencing of PLS3 in MDA-MB-231 triple-negative breast cancer cells increased the sensitivity towards paclitaxel, an anti-cancer agent.[31]

The role of PLS3 in the leader cell function of basal-like cells during collective invasion remains to be elucidated. Using the MMTV-PyMT breast cancer organoid model we

studied this relation. We first determined the protein distribution of PLS3 in luminal and basal-like cells in MMTV-PyMT organoids, in 3D and 2D *in vitro* models with immunofluorescence and confocal microscopy. We next determined the functional role of PLS3 in invasion in 3D collagen 1 by knocking down PLS3 in our organoid model.

Material and methods

Organoid culture

MMTV-PyMT H7 organoid lines were cultured in 45µl drops of BME (RGF type 2 Path Clear) from Bio-Techne. The growth medium used was Dulbecco's Modified Eagle Medium F12 (Gibco), enriched with one percent of HEPES (Gibco), Pen-Strep (Lonza) and glutamax 100X (Gibco) and supplemented with N-Acetyl-L-Cysteine (Sigma), Primocin (Bio-Connect), B27 (Thermo Fisher) and human fibroblast growth factor 2 and refreshed every other day.

Embedding organoids in 3D matrices

Organoids cultured in BME gels were collected using cold media, followed by treatment with dispase (Life Technology) to break down the remaining BME and consequently embedded in 45 µl drops of collagen 1 or BME gels on 24-well plates. The collagen 1 gels were prepared with 3.28 mg/ml rat tail collagen 1 from Corning, 10X phosphate buffered saline (PBS), MilliQ and NaOH which was submerged in ice for 2 hours at minimum. Subsequently, organoids in growth media were added and the mixture was left at room temperature (RT) for 5 minutes before plating. After plating of the collagen 1 and BME drops, the gels were flipped several times and left to polymerize at 37℃ upside down for at least 30 minutes. Subsequently 750µl of growth media was added and refreshed every other day.

Embedding organoids in 2D matrices

Collagen 1 coated cover glass was made as follows; collagen 1 solutions of 0.05 mg/ml rat tail type 1 collagen in 0.1% acetic acid was prepared and added onto the glass of 8-well chamber slides for 20 minutes at RT, removed, washed twice with PBS and left for drying. BME-coated glass was made likewise. Organoids cultured in BME gels were collected using cold media, followed by treatment with dispase (Life Technology), to break down the remaining BME, and added onto the covered glass.

Antibodies and reagents

Primary antibodies used for immunofluorescence were plastin 3 (100 µg) (rabbit, cat# PA5-98063) from Thermo Fisher, keratin 8 (33µM) (rat, cat#531826) from Developmental Studies Hydridoma Bank and keratin 14 (3.3µM) (rabbit, cat#905301) from Biolegend. The secondary antibodies used were Alexa Fluor goat anti-mouse 488, goat anti-rat 647 and goat anti-rabbit 568 (2µM) as well as 4′,6-diamidino-2-phenylindole (DAPI) (20µM) and all were obtained from Thermo Fisher. For f-actin visualization, 568-conjugated phalloidin (10µM) (Invitrogen) was used. Primary antibodies used for western blot were against plastin 3 (100 µg) (Thermo Fisher, rabbit, cat# PA5-98063), actin (0.4µM) (Millipore, mouse, cat#1501), and keratin 14 (1µM) (Abcam, mouse, cat#ab7800). The secondary western blot antibodies were Odyssey goat anti-mouse 800 and goat anti-rabbit 680 (0.4µM each).

Immunofluorescence and confocal imaging

Collagen 1 gels were fixed for 10 to 15 minutes by 4 percent paraformaldehyde in 1X PBS at RT followed by a washing step with 1X PBS. BME gels were fixed similarly but were embedded in collagen 1 after fixation. Samples were submerged in 1X PBS and stored in 4°C. Collagen 1- and BME-coated lab techs were also fixed with 4 percent paraformaldehyde in 1x PBS and washed with 1X PBS.

For immunostaining, the gels were gathered from the well-plates and transferred into 1.5 mL Eppendorf tubes wherein blocking was done using Normal Goat Serum (10 %) dissolved in PBS with 0.3 percent Triton for 1

hour while shaking at RT. After blocking, a solution of the primary antibodies in PBS with 0.1 percent Bovine Serum Albumin (BSA) from Sigma Life Sciences was added at 4°C for a minimum of 18 hours while shaken. The samples were washed 4 times with PBS for at least 10 minutes per wash while shaken. The same was done for the secondary antibodies. Consequently, samples were imaged on WillCo Wells (WillCo Well BV) with a glass bottom using a confocal microscope (LSM 880 Zeiss) with an 40X magnification objective and an NA of 1.1.

Quantification immunofluorescence signal in confocal images 3D

Quantification of PLS3 and K14 signal in organoids invading in 3D collagen 1 was done using confocal images from 40x objective. Cells within the organoids were classified as leader cells if they were at the tip of a protrusive strand. Cells were classified as rim cells if they were non-protrusive and localized at the outer cellular layer of the organoid (the layer forming the organoid-ECM interface). Using ImageJ, leader and rim cells were selected randomly. A minimum of 4 rim cells per organoid and all leader cells that were present in one organoid, were used. Cells needed to be fully in focus. Regions of interests (ROIs) were drawn around the cytosol (excluding the nucleus) of the cell and the mean grey value was measured. Background signal, from ROIs drawn of regions in the images that did not contain cells, (mean grey value of +/- 1.0) was subtracted from the mean grey values from the cytosols.

Quantification immunofluorescence signal in confocal images 2D

Quantification of the 2D images was manually done. Cells that were analyzed were always fully in focus. Cells were classified as K14/PLS3 negative or positive. Cells were considered K14-positive if they showed a filamentous signal in the cytosol and K14-negative if the cells did not show this signal. Cells were classified as PLS3-positive if they showed any fiber-like structures and were classified PLS3-negative if the cells did not contain any of these structures.

Doxycyclin inducible plastin3 knockdown generation and plastin3 knockdown experiments

Four independent shRNAs were used to construct four different knockdown clones. Plastin3-1-FWD: tgatagagatACCGGGCTCAATCAAATCGCACCGAACTCGAGTTCGGTGCGATTTGATTGAGCTTTTTtcgagacgcgtccta; Plastin3-1-REV:taggacgcgtctcgaAAAAAGCTCAATCAAATCGCACCGAACTCGAGTTCGGTGCGATTTGATTGAGCCCGGTatctctatca; Plastin3-2-FWD:tgatagagatACCGGCGGATATAAAGTGAGAGAAATCTCGAGATTTCTCTCACTTTATATCCGTTTTTTcgagacgcgtccta; Plastin3-2-REV:taggacgcgtctcgaAAAAACGGATATAAAGTGAGAGAAATCTCGAGATTTCTCTCACTTTATATCCGCCGGTatctctatca; Plastin3-3-FWD:tgatagagatACCGGGCTCAGAATTTAGACGGGAATCTCGAGATTCCCGTCTAAATTCTGAGCTTTTTtcgagacgcgtccta; Plastin3-3-REV: taggacgcgtctcgaAAAAAGCTCAGAATTTAGACGGGAATCTCGAGATTCCCGTCTAAATTCTGAGCCCGGTatctctatca; Plastin3-4-FWD: tgatagagatACCGGCCGGATATAAAGTGAGAGAAACTCGAGTTTCTCTCACTTTATATCCGGTTTTTTcgagacgcgtccta; Plastin3-4-REV: taggacgcgtctcgaAAAAACCGGATATAAAGTGAGAGAAACTCGAGTTTCTCTCACTTTATATCCGGCCGGTatctctatca

These oligos were incorporated in a pLV FUTG Tetracycline inducible shRNA vector. Lentiviral particles containing the shRNA vectors were already established in the lab. Lentivirus was incubated with single cells of H7 organoids for 4 hours. Single cells were then grown in BME into organoids for couple of passages with the selection by the addition of 3.0 µg/ml blasticidin to the growth media. Induction of the shRNA was done by the pretreatment of the organoids with 0.5 µg/ml doxycyclin for 3

days. After priming, the organoids were transferred to different matrices for 3 days, where doxycyclin was again present in the growth media.

Collagen 1 invasion assays and quantification

Organoids were embedded in collagen 1 for 3 days and imaged for invasion count. 4x brightfield images were used in Fiji. In Fiji, a body was drawn surrounding the core of the organoid and from there a line was drawn until the end of a strand. From each line the length was measured in µm, corrected for pixel to µm ratio. A pointed strand was classified as a strand of which the point of the head of the strand was considerably smaller in width than at the beginning of the head. A blunt strand was classified as a strand of which the point of the head was not considerably smaller in width than the beginning of the head.

Western blot experiments

Confluent BME or collagen 1 gels were collected with cold 1xPBS and taken for centrifugation. Supernatant was removed and sample buffer was added. Samples were sonicated five times for 30 seconds at 4℃ and boiled for 5 minutes at 95℃. Afterwards, samples were loaded and ran through a 10% acrylamide gel for 90 minutes at 120 volts. The proteins were transferred into an IF-PVDF membrane for 90 minutes at 0.35 Ampère. Blocking was done for 1 hour with 5% milk dissolved in TBS. Primary antibodies were dissolved in 5% BSA in TBS with 0.1% Tween overnight at 4℃. Washing was done 4 times with 10 ml TBST at RT. Secondary antibody incubation was done for 1 hour with shaking at RT, using the same antibody buffer as for the primary antibodies. Washing was done 4 times with 10 ml TBST at RT and membranes were stored in TBS. Imaging was done by an Amersham Typhoon scanner.

Western blot quantification

Quantification of western blot results was done using the program Image Studio Lite, version 4.0 by LI-COR. Knockdown efficiency was calculated as follows:

$$(R^{-dox} - R^{+dox}) / R^{-dox} \times 100\%$$

Where the R is the ratio between the PLS3 mean grey values divided by the corresponding Actin mean grey value.

Immunohistochemistry IDC samples

Paraffin-embedded, formalin-fixed breast cancer samples were selected from the Human Protein Atlas project. Samples were stained against PLS3 (HPA020433). From 7 samples, 2 were excluded due to bad quality (detached tissue from the slide). From the 5 samples, 3 showed multicellular invasive patterns.

Kaplan-Meier plot

Kaplan-Meier plot was derived from Balázs Győrffy et al.[32]

Statistical analysis

Statistical analysis was done for experiments that were conducted two or more times and was performed using GraphPad Prism 5. For comparisons between two groups, two-tailed Mann-Whitney U test with an alfa of 0.05 was used.

Results

PLS3 is expressed at the tumor-ECM interface in multicellular invasive structures in IDCs

To investigate the distribution of PLS3 in breast cancer tissues and the clinical relevance, we looked at immunohistochemistry stainings from the Human Protein Atlas of PLS3 in IDC tissue samples (Fig. 1). We selected the IDC samples that showed multicellular invasive patterns extending into the breast tissue (Fig. 1a-c, zoom in). The multicellular invasive patterns are reminiscent of collective invasion and were detected in 3 of the 5 IDC tissue sections analyzed. In 1 of the 3 samples, the cancer cells within the multicellular invasive patterns were negative for PLS3 (Fig. 1a zoom in, black arrows). In this sample high signal of PLS3 was detected in the stromal cells (Fig. 1a zoom in, black arrowheads). Morphology was hard to determine, but these cells could resemble immune cells (rounded morphology) or fibroblasts (spindle shaped). In the other two samples, PLS3 was detected in the stromal fibroblasts (Fig. 1biii, black arrowheads) and interestingly in the cells forming the ECM-interface of the invasive strands that may represent the leader cells of invasion (Fig. 1bi, bii, black arrowheads). Occasionally, we found tumor cells organized in *in situ*-like morphology, there high levels of PLS3 were detected in cancer cells forming the tumor-ECM interface (Fig. 1ci, arrowheads). Thus, PLS3 is expressed in cells forming the ECM interface of the collective invasion strands in IDC patients. In addition, survival analysis of the entire transcriptome in 4929 breast cancer patients by Balázs Győrffy et al.[32], revealed that patients with a high mRNA expression of PLS3 in the primary breast tumors had a worse relapse-free survival rate than patients with a low expression of PLS3 (Fig.1d). The association of PLS3 expression with poor clinical outcome, suggest possible involvement of PLS3 in promoting tumor progression in patients.

PLS3 is more expressed in basal-like cells and is enriched in leader cells

To study PLS3 *in vitro* in an invasive organoid model, we embedded H7 organoids in collagen 1 for 3 days, after which they were fixed in PFA and immunostained for PLS3, K14, K8 and DAPI. Basal-like cells (high in K14 and low in K8 expression) were predominantly located to the outer layer of the organoid that makes contact with the ECM, rim cells (Fig.2a). Luminal-like cells (low in K14 and high in K8 expression) were predominantly surrounded by basal-like cells. PLS3 expression was seen in all the cells at the organoid-ECM interface. We next distinguished between rim cells as either K14 high or K14 low-expressing, set by a threshold based on the overall mean of K14 expression in rim cells. PLS3 expression was higher in the rim cells that were high in K14 compared to rim cells that were low in K14 (Fig.2b). To confirm this, we calculated whether the expression of PLS3 was correlated with K14 levels in rim cells. Indeed, a Pearson's correlation test showed that K14 and PLS3 expression are moderately correlated in rim cells (Fig.2c). In addition, PLS3 expression was even more enriched in basal-like leader cells compared to any cells that were at the rim (Fig.2b).
In summary two conclusions can be drawn from this data: PLS3 is more expressed at the organoid-ECM interface in basal-like cells high in K14 (1) and PLS3 expression is enriched in leader cells compared to rim cells (2). This is in line with previous seen IDC images, where PLS3 is distributed along the tumor-ECM interface.

Since a correlation of basal-like cells and PLS3 expression was found in above-mentioned 3D experiments, we tried to find the same correlation in a simpler 2D model. Organoids were taken out of their 3D medium and plated onto 2D collagen 1-covered cover glass for 3 days, after which they were fixed with PFA and confocal images were made and are shown in figure 3a. PLS3 localization was mostly restricted to cells that were in the leading edge, in these formed lamellipodia and

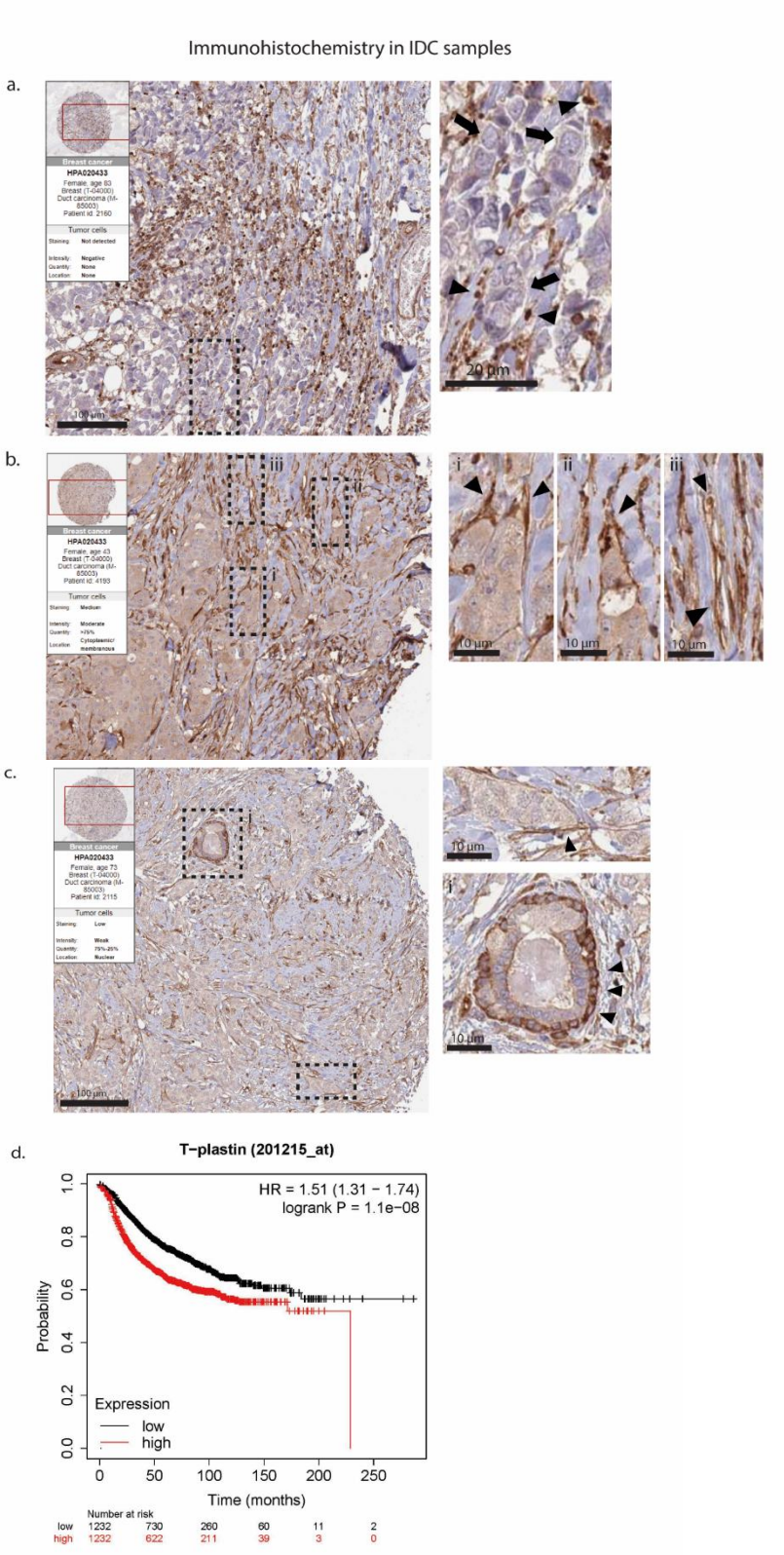

Figure 1 – IHC of PLS3 in invasive multicellular strands in IDCs and its relation to relapse-free survival rate in breast cancer patients. (a-c) 3 out of 5 selected IDCs with multicellular invasive structures. (d) Kaplan-Meier plot showing the correlation between relapse-free survival and the mRNA expression levels of PLS3. Patients were divided based on low expression levels of PLS3 (black) and high expression levels of PLS3 (red), where the media was used as a threshold. Data derived from the analysis of entire transcriptomes in 4929 breast cancer patients. Hazard ratio (HR) of 1.51 was found.

filamentous fiber-like structures aligned with the direction of cell movement, highlighting the stress fibers seen in the F-actin stainings. The PLS3 signal mostly came from lower z-stacks, suggesting that PLS3 allocates to parts of the cell that make contact with the ECM. Thus, PLS3 expression in this 2D model is also located to the organoid-ECM interface, as in the 3D organoid model. K14 expression was seen as cotton-like structures and located to either cell that were in the leading edge as well as cells in the center of the organoid. Of 27 selected cells in the leading edge, 19 were simultaneously positive for PLS3 as for K14 and 5 were simultaneously negative for PLS3 and K14 (Fig. 3b). This suggest that the relationship

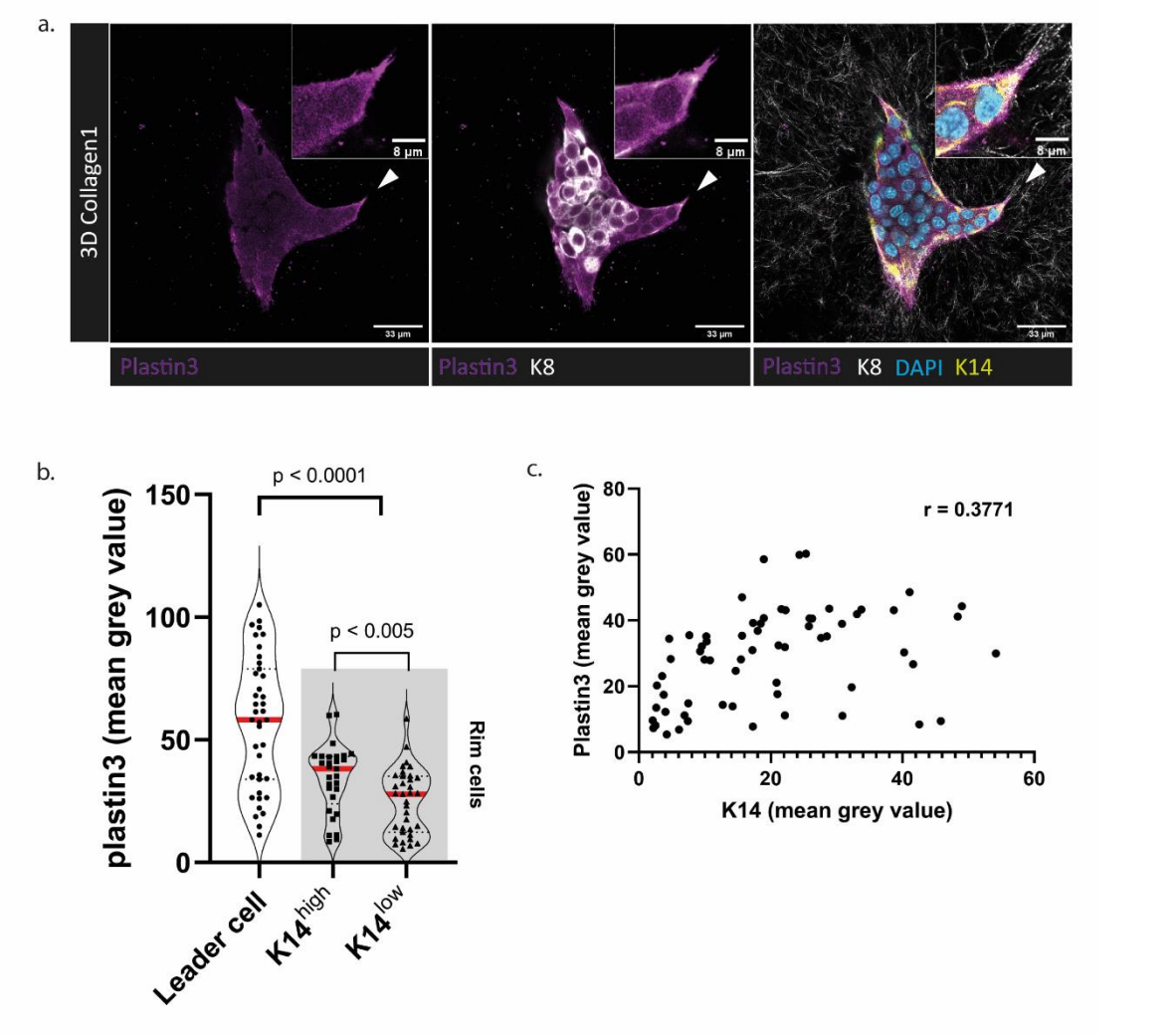

Figure 2 - PLS3 localization in invasive organoids and its relation to K14 expression (a) Confocal image of an organoid 3 days in collagen 1, stained for PLS3, K8, K14 and DAPI. Arrowheads indicate a leader cell. (b) PLS3 expression in leader cells, $K14^{high}$ rim cells and $K14^{low}$ rim cells. Data points from rim cells were split into a $K14^{high}$ and $K14^{low}$ group based on the mean of the K14 expression levels. (c) Pearson's correlation graph between PLS3 and K14 in rim cells. Data represents individual cells (dots) with median (red line) derived from two independent experiments with 17 organoids in total (n=2). 39 leader cells and 64 rim cells were used for quantification. The mean grey value of PLS and K14 in the cytosol were corrected for background signal. Cells were classified as leader cells if they were at the tip of a formed protrusive strand. Cells were classified as rim cells if they were non-protrusive and localized to the body of the organoids. P-values, two-tailed Mann-Whitney test.

between basal-like cells and PLS3 expression also applies in this 2D model.

In summary, both models show that PLS3 expression is located to the organoid-ECM interface, which is in line with the IDC images, and that PLS3 expression is basal-like cell associated and even upregulated in leader cells in 3D, which in turn is in line with our previously done single cell mRNA sequencing data that showed that PLS3 is upregulated in basal-like cells in organoids in collagen 1.

a.

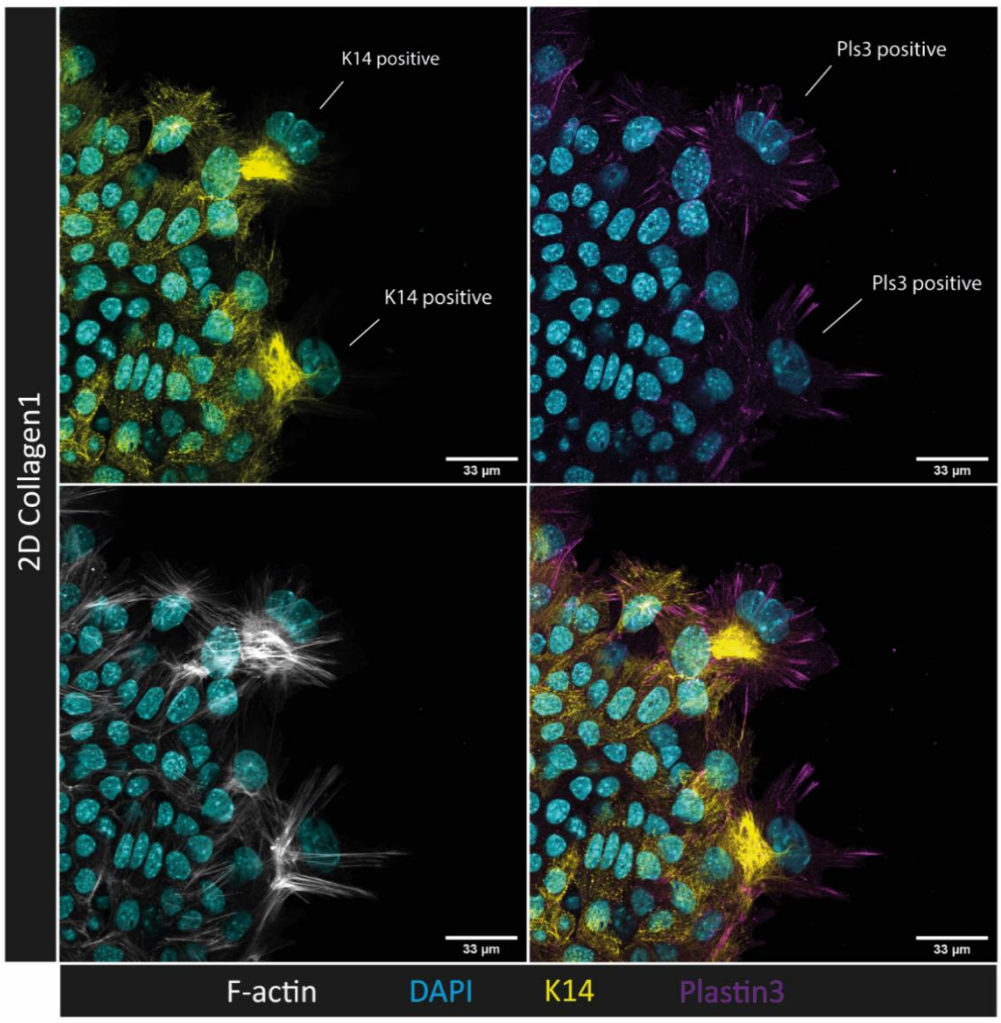

b.

Leading edge cells

		PLS3		
		+	-	total
K14	+	19	1	20
	-	2	5	7
	total	21	6	27

Figure 3 – PLS3 localization and its relation to K14 expression in 2D (a) Maximum projection of confocal images of organoids 3 days on collagen-covered cover glass immunostained for PLS3, F-actin, K14 and DAPI. (b) Table of selected cells in the leading edge that were classified based on PLS3 and K14 expression. Data is derived from one experiment with 27 cells from 8 organoids (n=1).

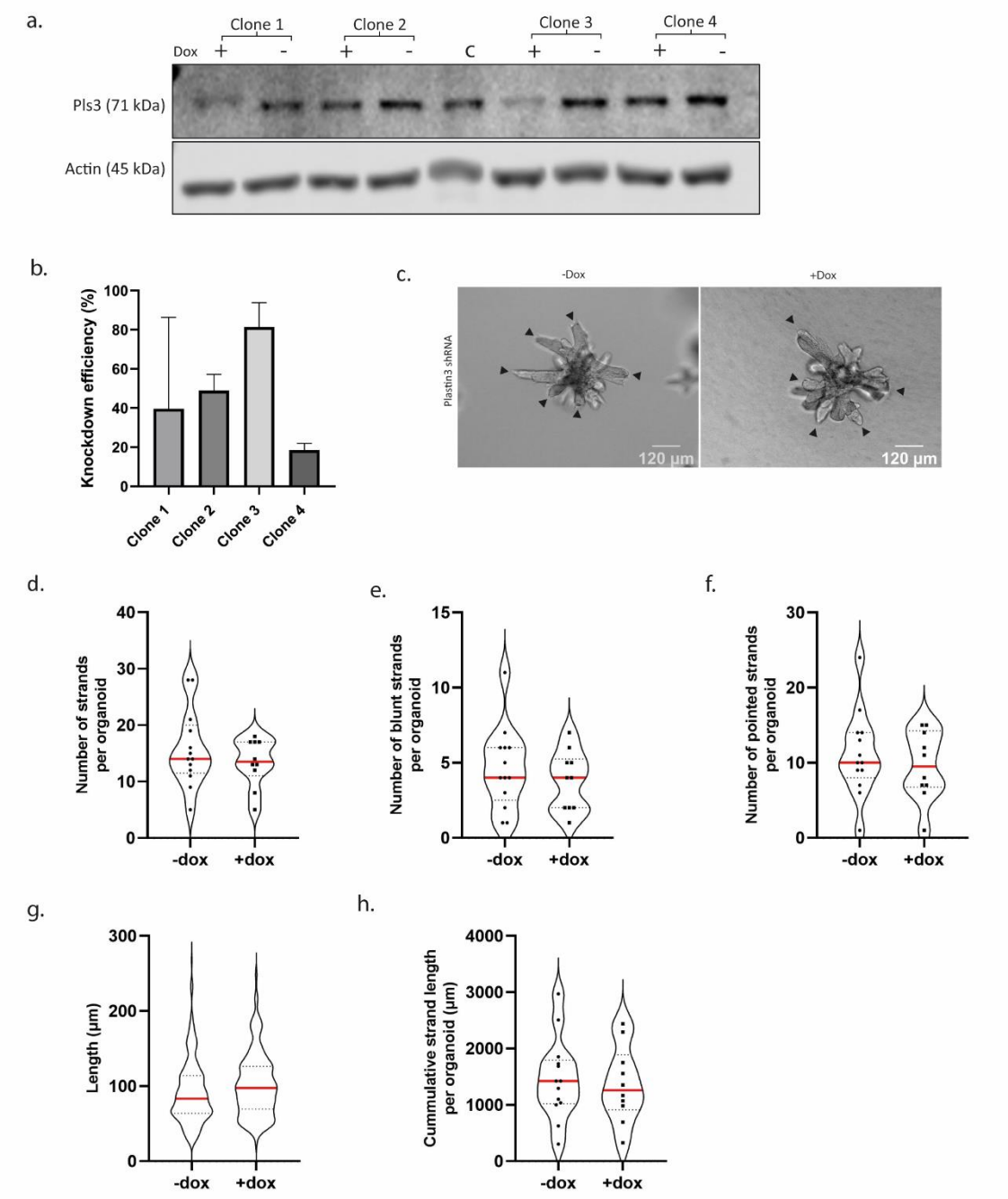

Figure 4 – Downregulation of PLS3 does not affect invasion. (a) Western blot of the four different PLS3-knockdown clones in the presence and absence of doxycyclin. Gels were stained for PLS3 (71 kDa) and Actin (45 kDa). C=control. Four independent dox-inducible shRNA sequences were used. (b) Bar graph of knockdown efficiency per clone in BME. Average knockdown efficiencies were: 30.85% (clone 1), 48.92% (clone 2), 81.41% (clone 3) and 18.55% (clone 4) (c) Brightfield image of clone 3 organoid in collagen 1 in the absence (left) and presence (right) of doxycyclin. Arrowheads indicate invasive strands. (d) Number of strands per organoid. (e) Number of blunt strands per organoid. (f) Number of pointed strands per organoid. (g) Length of strands per organoid. (h) Cumulative strand length per organoid. Data points are collected from one experiment with 13 -dox organoids and 10 +dox organoids. In the collagen experiment (c), knockdown efficiency was determined at 61.8% by western blot analysis.

PLS3 downregulation does not affect the formation of protrusive strands in collagen 1

In order to investigate whether PLS3 is essential for invasion, we established four MMTV-PyMT organoid lines expressing different PLS3 shRNA sequences (Fig. 4a). From these organoid lines, clone 3 showed the highest knockdown efficiency of 81.41% (Fig. 4b), after which this organoid line was used to perform functional studies. Organoids were first grown for 3 days with doxycycline in BME and then put in collagen 1 for an extra 3 days (in the presence of doxycycline), after which invasion was quantified. Knockdown efficiency in collagen 1 was 61.81%. In both conditions, -dox and +dox, invasive strands were formed (Fig. 4c). However, the number of strands per organoid did not chance when PLS3 was knocked down (Fig.4def). As well as the length of the strands did not chance in the knocking down of PLS3 (Fig. 4g). Likewise, cumulative strand length per organoid did not chance when PLS3 was knocked down (Fig. 4h). Thus, the downregulation of PLS3 does not affect invasion. However, whether these strands are fully PLS3 negative needs to be confirmed by IF.

Discussion

Basal-like cells have an important role to play in the initiation and guidance of collective invasion. Using the MMTV-PyMT 3D *in vitro* model, we found that PLS3 expression is upregulated in basal-like cells, especially when they are the leader cells of invasive multicellular strands. Furthermore, we show that partial knockdown of PLS3 does not affect invasion, leaving the role of PLS3 in leader cells and collective invasion an open question that needs to be further studied.

Luminal cancer cells acquire a basal epithelial program in order to become invasive (Cheung et al).[12] Data from single cell mRNA sequencing previously done in our lab, showed that PLS3 is upregulated in basal-like leader cells in collagen 1 compared to BME. Moreover, immunohistochemistry images from the Human Protein Atlas project show that PLS3 is expressed in cells forming the tumor-ECM interface of collective invasive strands in IDC patients. Whether these PLS3-positive cells at the tumor-ECM interface are cancer cells or stromal cells, remains to be investigated.

This could be done by co-staining PLS3 in IDCs with additional markers for cancer and stromal cells, such as K8/K14 and vimentin, respectively. Our work *in vitro* shows that PLS3 expression is enriched in cytoplasmic protrusions of basal-like leader cells in 3D. Moreover, we show that PLS3 locates at close proximity with F-actin associated stress fibers at the leading edge in 2D. This all suggests a potential role for PLS3 in driving collective invasion.

PLS3 may contribute to collective invasion by regulating cytoskeleton protrusions, which are essential to leader cell function. PLS3's association with filopodia formation has been described in detail[19,33,34]. PLS3 is highly localized in filopodia at the distal portion of actin filaments where PLS3 bundles the filaments together, making the actin filaments parallel to the direction of tension.[21] In addition, it has been described that PLS3 reinforces membrane protrusions to bridge matrix gaps during cell migration.[23] Furthermore, PLS3 promoted cell migration may play a role in ECM remodeling, which is important during invasion. Dor-On et al state that PLS3 is involved in the assembly of the basement membrane in mice epidermis.[35] This means that PLS3 could play a putative role in ECM remodeling, which is important during invasion. Since this is not studied in collagen 1 yet, further research the role of PLS3 in collagen 1 remodeling still needs to be done.

Interestingly, the knocking down of PLS3 in our breast cancer MMTV-PyMT 3D model did not show an effect on invasion. These experiments still lack full confirmation that the invading leader cells are indeed reduced in PLS3 protein level. This could be done by

immunofluorescence after PLS3-knockdown, for example. However, the leader cells still contain 40% of its normal amount of PLS3 protein, so a full knockout would be a better way to study this.

In addition, the contribution of PLS3 to leader cell function could be a small part in a bigger cascade. It has been described that PLS3 is involved in the p38 mitogen-activated protein kinase (MAPK) signaling pathway.[31] In addition, PLS3 seems to be a regulator in the PI3K/Akt signaling pathway.[36] So it could be that downregulation of PLS3 will not show an immediate effect. Further experiments with perhaps various timepoints in knockdown would be a way to study this.

On the other hand, the potential pro-invasive effect of PLS3 might not take place in the 3D collagen 1 model that is used in our experiments (with only small gaps in the collagen 1 fibers). Garbett D. et al showed that PLS3 reinforces membrane protrusions when there are big gaps between ECM and was mostly characterized on 2D fibronectin models. So, in the future it would be interesting to study PLS3 in our organoids in a 2D fibronectin model an in 3D gels with bigger pores.

Nonetheless, PLS3 expression shows potential as a diagnostic and prognostic biomarker in breast cancer. Likewise, the Kaplan-Meier plot in figure 2 of Balázs Győrffy et al shows that high expression of PLS3 is disadvantageous for relapse-free survival compared to low expression of PLS3.[32] Research done by Ueo et al found that PLS3 is a suitable prognostic marker in circulating tumor cells (CTCs) in breast cancer patients.[30] Thus, PLS3 might be involved in early and late steps of the metastatic cascade. Moreover, Yan Ma et al found that PLS3 downregulation in the human breast cancer cell line MDA-MB-231, results in an increased sensibility towards the anti-cancer agent paclitaxel (PTX).[37] A change in the p38 MAPK-signaling pathway seemed to be the cause. As well as in liver cancer, downregulation of PLS3 increases the sensitivity to cisplatin, a chemotherapeutic cancer drug.[29] Thus, PLS3 may promote multiple aggressive cellular behavior including cancer cell invasion and survival and contribute by that to carcinogenesis and metastasis.

In conclusion, these data provide initial molecular insight on the actin-rich protrusions of basal-like cells that drive collective invasion. In addition, this work sets the stage for further investigation to test the use of PLS3 as a marker for the invasive fronts of epithelial tumors in general and breast tumors in particular.

Acknowledgements

I would like to deeply thank Antoine A. Khalil for his excellent guidance, endless patience and support during my project and Johan de Rooij for allowing me to do my major internship in his group. I would also like to thank the Martijn Gloerich group and Patrick Derksen group for their helpful insights.

References

1. Jesinger, R. A. Breast Anatomy for the Interventionalist. (2014) doi:10.1053/j.tvir.2013.12.002.
2. Keller, P. J. *et al.* Defining the cellular precursors to human breast cancer. doi:10.1073/pnas.1017626108.
3. Mak, K. M. & Mei, R. Basement Membrane Type IV Collagen and Laminin: An Overview of Their Biology and Value as Fibrosis Biomarkers of Liver Disease. *Anat. Rec.* **300**, 1371–1390 (2017).
4. Klinge, U. *et al.* Expression of the extracellular matrix proteins collagen I, collagen III and fibronectin and matrix metalloproteinase-1 and -13 in the skin of patients with inguinal hernia. *Eur. Surg. Res.* **31**, 480–490 (1999).
5. Srivastava, V., Huycke, T. R., Phong, K. T. & Gartner, Z. J. Organoid models for mammary gland dynamics and breast cancer. *Curr. Opin. Cell Biol.* **2020**, 51–58 (2020).
6. Europa Donna » Breast Cancer Facts. https://www.europadonna.org/breast-cancer-facs/.
7. Weigelt, B. & Bissell, M. J. Unraveling the microenvironmental influences on the normal mammary gland and breast cancer. *Semin. Cancer Biol.* **18**, 311–321 (2008).
8. Hein, S. M. *et al.* Luminal epithelial cells within the mammary gland can produce basal cells upon oncogenic stress. (2016) doi:10.1038/onc.2015.206.
9. The transition from hyperplasia to invasive carcinoma of the breast. https://onlinelibrary-wiley-com.proxy.library.uu.nl/doi/epdf/10.1002/%28SICI%291096-9896%28199902%29187%3A3%3C272%3A%3AAID-PATH265%3E3.0.CO%3B2-2.
10. Wiechmann, L. & Kuerer, H. M. The molecular journey from ductal carcinoma in situ to invasive breast cancer. *Cancer* **112**, 2130–2142 (2008).
11. Place, A. E., Jin Huh, S. & Polyak, K. The microenvironment in breast cancer progression: Biology and implications for treatment. *Breast Cancer Res.* **13**, 1–11 (2011).
12. Cheung, K. J., Gabrielson, E., Werb, Z. & Ewald, A. J. Collective Invasion in Breast Cancer Requires a Conserved Basal Epithelial Program. (2013) doi:10.1016/j.cell.2013.11.029.
13. Friedl, P., Locker, J., Sahai, E. & Segall, J. E. R E V I E W Classifying collective cancer cell invasion. *Nat. Cell Biol.* (2012) doi:10.1038/ncb2548.
14. Khalil, A. A. & Friedl, P. Determinants of leader cells in collective cell migrationw. *This J. is* **2**, 568–574 (2010).
15. Khalil, A. A. & de Rooij, J. Cadherin mechanotransduction in leader-follower cell specification during collective migration. *Exp. Cell Res.* **376**, 86–91 (2019).
16. Khalil, A. A. *et al.* Collective invasion in ductal and lobular breast cancer associates with distant metastasis. *Clin. Exp. Metastasis* **34**, 421–429 (2017).
17. Bronsert, P. *et al.* Cancer cell invasion and EMT marker expression: a three-dimensional study of the human cancer-host interface. *J. Pathol.* **234**, 410–422 (2014).
18. Lin$, C.-S., Park$, T., Chen$, Z. P. & Leavitt$$, J. THE JOURNAL OF BIOLOGICAL CHEMISTRY Human Plastin Genes COMPARATIVE GENE STRUCTURE, CHROMOSOME LOCATION, AND DIFFERENTIAL EXPRESSION IN NORMAL AND NEOPLASTIC CELLS*. **268**, 2781–2792 (1993).
19. Bretscher, A. Fimbrin is a cytoskeletal protein that crosslinks F-actin in vitro. *Proc. Natl. Acad. Sci.* **78**, 6849–6853 (1981).

20. Wolff, L. *et al.* Plastin 3 in health and disease: a matter of balance. *Cell. Mol. Life Sci.* **78**, 5275–5301 (2021).

21. Xue, F., Janzen, D. M. & Knecht, D. A. Contribution of Filopodia to Cell Migration: A Mechanical Link between Protrusion and Contraction. *Int. J. Cell Biol.* **2010**, 13 (2010).

22. Schwebach, C. L. *et al.* ARTICLE Osteogenesis imperfecta mutations in plastin 3 lead to impaired calcium regulation of actin bundling. doi:10.1038/s41413-020-0095-2.

23. Garbett, D. *et al.* T-Plastin reinforces membrane protrusions to bridge matrix gaps during cell migration. doi:10.1038/s41467-020-18586-3.

24. Case, L. B. & Waterman, C. M. R E V I E W Integration of actin dynamics and cell adhesion by a three-dimensional, mechanosensitive molecular clutch. *Nat. Publ. Gr.* **17**, (2015).

25. van Dijk, F. S. *et al.* PLS3 Mutations in X-Linked Osteoporosis with Fractures . *N. Engl. J. Med.* **369**, 1529–1536 (2013).

26. Sugimachi, K. *et al.* Aberrant Expression of Plastin-3 Via Copy Number Gain Induces the Epithelial–Mesenchymal Transition in Circulating Colorectal Cancer Cells. *Ann. Surg. Oncol.* **21**, 3680–3690 (2014).

27. Kurashige, J. *et al.* Plastin3 is associated with epithelial-mesenchymal transition and poor prognosis in gastric cancer. *Oncol. Lett.* **17**, 2393–2399 (2019).

28. KURIYAMA, K. *et al.* Plasma plastin-3: A tumor marker in patients with non-small-cell lung cancer treated with nivolumab. *Oncol. Lett.* **21**, 1–1 (2021).

29. Ikeda, H. *et al.* The role of T-fimbrin in the response to DNA damage: Silencing of T-fimbrin by small interfering RNA sensitizes human liver cancer cells to DNA-damaging agents. *Int. J. Oncol.* **27**, 933–940 (2005).

30. Ueo, H. *et al.* Circulating tumour cell-derived plastin3 is a novel marker for predicting long-term prognosis in patients with breast cancer. *Br. J. Cancer* (2015) doi:10.1038/bjc.2015.132.

31. Ma, Y. *et al.* Plastin 3 down-regulation augments the sensitivity of mda-mb-231 cells to paclitaxel via the p38 mapk signalling pathway. *Artif. Cells, Nanomedicine Biotechnol.* **47**, 685–695 (2019).

32. Gy, B. & Orffy, }. Survival analysis across the entire transcriptome identifies biomarkers with the highest prognostic power in breast cancer. (2021) doi:10.1016/j.csbj.2021.07.014.

33. Giganti, A. *et al.* Actin-filament cross-linking protein T-plastin increases Arp2/3-mediated actin-based movement. *J. Cell Sci.* **118**, 1255–1265 (2005).

34. Bretscher, A. & Weber, K. Fimbrin, a new microfilament-associated protein present in microvilli and other cell surface structures. *J. Cell Biol.* **86**, 335–340 (1980).

35. Dor-On, E. *et al.* T-plastin is essential for basement membrane assembly and epidermal morphogenesis. *Sci. Signal.* **10**, (2017).

36. Xin, Z. *et al.* PLS3 predicts poor prognosis in pancreatic cancer and promotes cancer cell proliferation via PI3K/AKT signaling. *J. Cell. Physiol.* **235**, 8416–8423 (2020).

37. Journal, A. I. *et al.* Artificial Cells, Nanomedicine, and Biotechnology Plastin 3 down-regulation augments the sensitivity of MDA-MB-231 cells to paclitaxel via the p38 MAPK signalling pathway Plastin 3 down-regulation augments the sensitivity of MDA-MB-231 cells to paclitaxel. (2019) doi:10.1080/21691401.2019.1576707.